

## Morphology Investigation of Stereoblock Polypropylene Elastomer

Raisa L. Kravchenko,\* Bryan B. Sauer,  
R. Scott McLean, Mimi Y. Keating,  
Patricia M. Cotts, and Young H. Kim

DuPont, Central Research and Development,  
Experimental Station, Wilmington, Delaware 19880

Received September 13, 1999

Semicrystalline polypropylene (PP) containing both stereoregular isotactic and random atactic sequences belongs to an important class of thermoplastic elastomers. The isotactic segments in this polymer can crystallize forming physical cross-links while the atactic segments serve as a continuous amorphous phase.<sup>1,2</sup> Various synthetic methods have been developed for the preparation of this material using both heterogeneous Ziegler–Natta (ZN)<sup>1–4</sup> and homogeneous metallocene<sup>5–8</sup> catalysts. Polymers produced with heterogeneous catalysts tend to have broad molecular weight and tacticity distributions,<sup>3,4</sup> while those generated with homogeneous bridged metallocenes are much more uniform.<sup>6,9</sup> Elastomeric polypropylenes derived from the unbridged bis(2-arylindenyl) metallocenes<sup>7,10</sup> are intermediate between the other two types: they can be separated into several fractions of different tacticity and crystallinity,<sup>11–13</sup> but in contrast to polymers produced with heterogeneous ZN catalysts,<sup>3,4</sup> these fractions do not vary strongly in their molecular weight. The proposed “oscillating” mechanism for the stereoblock formation with bis(2-arylindenyl) metallocenes involves catalyst isomerization between an isospecific and an aspecific conformation during the growth of a single polymer chain resulting into isotactic and atactic sequences, respectively.<sup>7</sup> The presence of at least two types of active species during polymerization may account for the heterogeneity of produced polymers.<sup>12</sup> Studies of polypropylenes generated with the “oscillating” catalysts by differential scanning calorimetry (DSC) and optical depolarization techniques reveal broad melting transitions and the presence of fast and slow crystallization regimes possibly related to the coexistence of crystallizable sequences of different lengths.<sup>11,12</sup> However, no experimental measurements of the hard segment block lengths have been attempted so far. To better understand the domain structure of elastomeric polypropylenes derived from bis(2-arylindenyl) metallocenes, we have investigated the thermal properties and morphology of the crystalline domains of these materials using thermal fractionation DSC, atomic force microscopy (AFM), and nitric acid digestion in combination with analysis by gel permeation chromatography (GPC).

Polymerizations were conducted following a literature procedure at 23–25 °C in liquid propylene with bis(2-phenylindenyl)zirconium dichloride/methylaluminumoxane as catalyst.<sup>14</sup> The resulting polypropylene samples had isotactic pentad contents % *mmmm* = 25–30% (<sup>13</sup>C NMR),<sup>15,16</sup>  $M_w$  = 240 000–260 000, and molecular weight distributions ranging from 2.7 to 4.4 (determined by

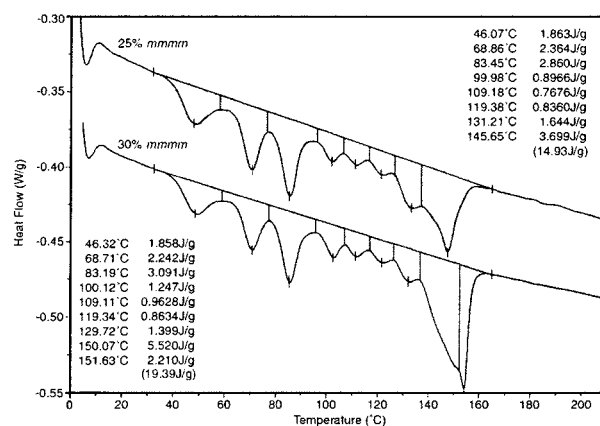


**Figure 1.** Thermal fractionation DSC curves for two elastomeric polypropylene samples with % *mmmm* = 25 and 30. The polymers were annealed in a DSC cell in a stepwise manner between 160 and 50 °C with 10 °C intervals and then reheated to obtain the melting profiles.

GPC). Polymers used in acid digestion studies were purified from alumina by extraction with refluxing xylenes.

Several DSC techniques were used for thermal characterization of the polymers. Melting temperatures and enthalpies of fusion were determined by heating samples from –50 to 200 °C at 10 °C/min. In agreement with the previously reported results,<sup>12</sup> broad melting endotherms with two melting peaks at 48 and 150 °C were observed for the samples aged at room temperature for at least 20 h. The low melting peaks were absent in melt quenched samples. Temperature-modulated DSC curves<sup>17</sup> exhibited an exotherm at 130 °C preceding the final melting endotherm at 150 °C, which suggested that the higher melting peak was at least partially due to recrystallization of lower melting crystallites into more perfect crystals during the scan.

To further characterize the crystallite size distribution and possibly the relationship to chain architecture and block lengths, we used the thermal fractionation DSC technique for two elastomeric polypropylene samples with slightly different isotacticities (% *mmmm* = 25 and 30). The polymers were crystallized in a DSC cell between 160 and 50 °C in a stepwise manner with 10 °C intervals. Samples were held for 12 h at each crystallization temperature to allow for equilibration and segregation of polymer fractions with similar crystallinities.<sup>18–21</sup> The curves shown in Figure 1 were obtained by reheating the stepwise annealed (thermally fractionated) samples. The melting profiles of the two samples were similar and showed the presence of many melting fractions. Sample with % *mmmm* = 30 contained a high melting fraction ( $T_m \approx 154$  °C), absent in the sample with % *mmmm* = 25, which was possibly related to the presence of longer isotactic sequences in the former polymer.<sup>21</sup> However, in addition to the influence of the block length of hard isotactic sequences, diffusion and kinetic limitations can restrict lamellar perfection, which prohibits one from quantitatively relating melting to chain structure only.

To characterize the domain structure of elastomeric polypropylene and its response to stress, we obtained AFM data in tapping mode (Nanoscope 3A, Digital

\* Corresponding author. e-mail: raisa.kravchenko@usa.dupont.com.

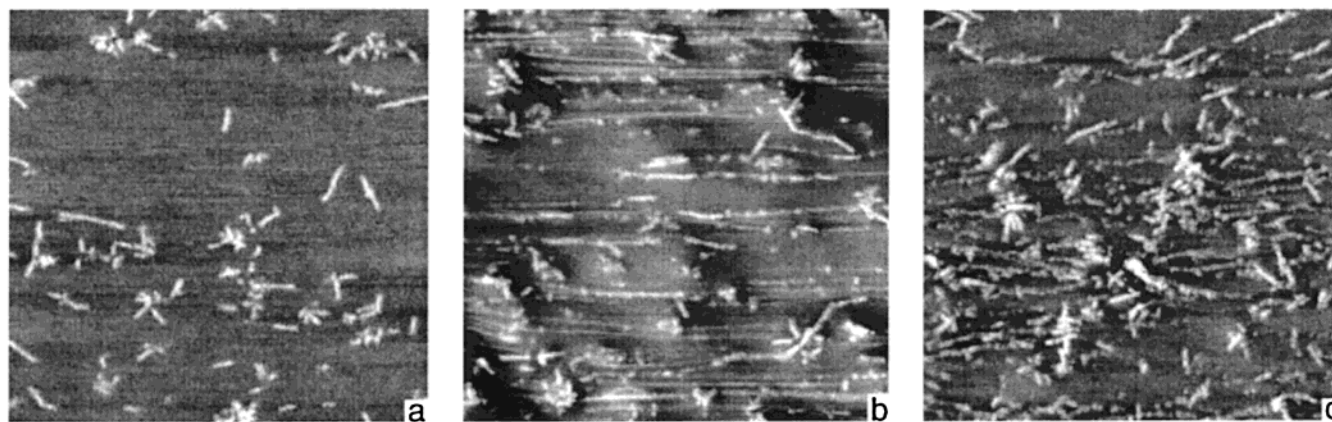


**Figure 2.** Atomic force microscopy phase data for a melt cast elastomer film. The scan boxes are all 1000 nm  $\times$  1000 nm, and the  $z$ -scale for the AFM phase lag is 0–20°: (a) an undeformed (1 $\times$ ) melt cast film annealed for 10 s at 80 °C and then cooled to room temperature for analysis; (b) a different region of the film after stretching to 8 $\times$ ; (c) the film relaxed to 4 $\times$  (a very low state of stress due to strain softening) after 8 $\times$  elongation.<sup>27</sup>

Instruments, Santa Barbara, CA) in air, using previously described methods.<sup>22,23</sup> Samples for AFM were prepared by casting films from a hot dichlorobenzene solution or melt pressing. Tapping mode is a contact technique, but the intermittent contact allows one to control the forces to very low levels and significantly reduce the lateral drag forces and surface damage compared to scanning “contact” AFM.<sup>22,23</sup> Here we present “phase lag” data which are sensitive to local stiffness differences of species or domains at or near the surface. Under our operating conditions,<sup>22,23</sup> hard domains have a larger phase lag and are plotted as the light regions. The AFM images of melt pressed and solution cast films appear similar and show dispersed anisotropic but discontinuous hard domains consisting of ribbonlike crystals immersed in a continuous softer amorphous phase (Figure 2a). The crystals are thin in two dimensions which is likely caused by the finite isotactic block lengths and the low crystalline segment fraction.<sup>24</sup> Infrared dichroism studies<sup>24</sup> of related aromatic polyester segmented elastomers have shown that the hard chain is oriented perpendicular to the length of the crystals. Since the morphology of our elastomeric polypropylene is similar for comparable hard segment fractions, we assume that the crystalline segment chains also traverse the crystal perpendicular to its long direction. The crystallite thickness measured normal to the long direction (Figure 2a) is  $12 \pm 4$  nm, which corresponds to about 54 propylene repeat units ( $M_n = 2270$ ).<sup>23,25,26</sup>

Typically these polypropylene elastomers have about 1000% elongation at break and tensile strength of up to 15 MPa.<sup>12,14</sup> This is a reasonably high tensile strength for such a high elongation material, but the stress–strain hysteresis is also large especially at deformations above 3 $\times$ .<sup>12,14,27</sup> To understand this, we obtained AFM data for films at a high strain. We found that almost all of the original crystallites were destroyed at high elongations (Figure 2b). The stress was sufficient to break up the initial ribbonlike crystals into small blocks contained mostly in fibrils. The mechanism of the crystallite breakup and orientation into fibrils may be similar to that of other segmented elastomers such as those with aromatic polyester<sup>26</sup> and polyamide<sup>23</sup> hard segments. The oriented nanofibrils in Figure 2b consist of an alternating structure of hard crystallites and possibly stress crystallized originally amorphous sequences with chains oriented in the strain direction in

both types of segments. Since AFM data are sensitive only to local stiffness contrast, lamellar crystals as well as stress crystallized or oriented soft segment could both be “stiff” enough to provide contrast. The hard crystallites in the fibrils are detected as the slightly wider regions and are better resolved in some fibrils than others possibly because of their different proximity to the surface which can influence AFM resolution. The hard domain physical cross-links support the amorphous orientation in these nanofibrils which are seen to span more than a few hundred nanometers in Figure 2b. The fibrils have a width in the narrow direction about half of the original lamellar thickness of 12 nm. Upon relaxation of stress, there is no re-formation of the initial morphology (Figure 2c). The oriented fibrils persist but with less directionality. For materials that exhibit high elongation and tensile strength, the load-bearing nanofibrils are important in structural reinforcement. The breakup of crystallites contributes to the large degree of strain hysteresis since this is essentially irreversible plastic deformation. At strains up to 3 $\times$  no substantial domain breakup has been detected by AFM, and strain hysteresis is also low.<sup>12</sup>

To further characterize the ELPP isotactic blocks, we attempted to isolate the crystalline segment by digesting the amorphous region in hot concentrated HNO<sub>3</sub>. As the acid is not able to penetrate tightly packed crystalline domains, it selectively digests the amorphous phase of the polymer.<sup>28</sup> Within 24 h at 80 °C, nearly 90% of the oriented film dissolved into nitric acid. The presence of 10% indigestible material is in good agreement with 10% crystallinity at 80 °C reported for this type of material in the literature.<sup>13</sup> After water and methanol washing of the undigested fraction, a powdery white precipitate soluble in THF was obtained. Analysis by GPC with light scattering detection showed that the powder had  $M_n = 4950$ , corresponding to degree of polymerization DP = 118, and narrow polydispersity  $M_w/M_n = 1.061$ . The thermal profile of the isolated fraction revealed a narrow melting transition at 131 °C and high enthalpy of melting (70 J/g). The difference in the crystallizable sequence lengths (118 repeat units) determined by this method and the one obtained from the AFM studies (54 repeat units) may be related to the unintentional digestion of smaller crystallites at 80 °C, leaving higher melting and thicker crystallites for GPC analysis. Possible chain folding of longer blocks combined with kinetic limitations of lamellar formation

would also explain the differences between the digestion and AFM determinations.

In conclusion, application of novel techniques to the study of thermoplastic elastomeric polypropylene derived from "oscillating" bis(2-phenylindenyl)zirconocene provided new information on the morphology of this material. Multiple melting fractions in the DSC scans of thermally fractionated samples characterized the polydispersity of the crystallizable block lengths. For the first time, we were able to observe crystal morphologies of these materials and their change during and after tensile extension using AFM. In addition, AFM and acid digestion studies provided the first experimental estimates of the crystallizable sequence lengths in these elastomers.

**Acknowledgment.** The authors thank S. Bair and J. Chen for laboratory assistance.

## References and Notes

- (1) Natta, G.; Mazzanti, G.; Crespi, G.; Moraglio, G. *Chim. Ind. (Milan)* **1957**, *39*, 275–283.
- (2) Natta, G. *J. Polym. Sci.* **1959**, *34*, 531–549.
- (3) Collette, J. W.; Tullock, C. W.; MacDonald, R. N.; Buck, W. H.; Su, A. C. L.; Harrell, J. R.; Mulhaupt, R.; Anderson, B. C. *Macromolecules* **1989**, *22*, 3851–3858.
- (4) Collette, J. W.; Ovenall, D. W.; Buck, W. H.; Ferguson, R. C. *Macromolecules* **1989**, *22*, 3858–3866.
- (5) Mallin, D. T.; Rausch, M. D.; Lin, Y. G.; Dong, S.; Chien, J. C. W. *J. Am. Chem. Soc.* **1990**, *112*, 2030–2031.
- (6) Gauthier, W. J.; Corrigan, J. F.; Taylor, N. J.; Collins, S. *Macromolecules* **1995**, *28*, 3771–3778.
- (7) Coates, G. W.; Waymouth, R. M. *Science* **1995**, *267*, 217–219.
- (8) Dietrich, U.; Hackmann, M.; Rieger, B.; Klinga, M.; Leskelae, M. *J. Am. Chem. Soc.* **1999**, *121*, 4348–4355.
- (9) Llinas, G. H.; Dong, S. H.; Mallin, D. T.; Rausch, M. D.; Lin, Y. G.; Winter, H. H.; Chien, J. C. W. *Macromolecules* **1992**, *25*, 1242–1253.
- (10) Hauptman, E.; Waymouth, R. M.; Ziller, J. W. *J. Am. Chem. Soc.* **1995**, *117*, 11586–11587.
- (11) Carlson, E. D.; Krejchi, M. T.; Shah, C. D.; Terakawa, T.; Waymouth, R. M.; Fuller, G. G. *Macromolecules* **1998**, *31*, 5343–5351.
- (12) Hu, Y.; Krejchi, M. T.; Shah, C. D.; Myers, C. L.; Waymouth, R. M. *Macromolecules* **1998**, *31*, 6908–6916.
- (13) Hu, Y.; Carlson, E. D.; Fuller, G. G.; Waymouth, R. M. *Macromolecules* **1999**, *32*, 3334–3340.
- (14) Kravchenko, R.; Masood, A.; Waymouth, R. M.; Myers, C. L. *J. Am. Chem. Soc.* **1998**, *120*, 2039–2046.
- (15) Zambelli, A.; Locatelli, P.; Bajo, G.; Bovey, F. A. *Macromolecules* **1975**, *8*, 687–689.
- (16) Bovey, F. A. *Chain Structure and Conformation of Macromolecules*; Academic Press: New York, 1982.
- (17) Reading, M. *Trends Polym. Sci.* **1993**, *1*, 248–253.
- (18) Keating, M. Y.; McCord, E. F. *Thermochim. Acta* **1994**, *243*, 129–145.
- (19) Keating, M.; Lee, I.-H.; Wong, C. S. *Thermochim. Acta* **1996**, *284*, 47–56.
- (20) Fu, Q.; Chiu, F.-C.; McCreight, K. W.; Guo, M.; Tseng, W. W.; Cheng, S. Z. D.; Keating, M. Y.; Hsieh, E. T.; DesLauriers, P. J. *J. Macromol. Sci., Phys.* **1997**, *B36*, 41–60.
- (21) Keating, M. Y.; Lee, I.-H. *J. Macromol. Sci., Phys.* **1999**, *B38*, 379–401.
- (22) Magonov, S. N.; Elings, V.; Whangbo, M.-H. *Surf. Sci.* **1997**, *375*, L385–L391.
- (23) McLean, R. S.; Sauer, B. B. *J. Polym. Sci., Polym. Phys.* **1999**, *37*, 859–866.
- (24) Lilaonitkul, A.; Cooper, S. L. *Rubber Chem. Technol.* **1977**, *50*, 1–23.
- (25) 6.7 Å per helical repeat containing three propylene units. Miller, R. L. In *Crystalline Olefin Polymers, Part I*; Raff, R. A. V., Doak, K. W., Eds.; John Wiley & Sons: New York, 1965; p 589.
- (26) Cella, R. J. *J. Polym. Sci., Polym. Symp.* **1973**, *42*, 727–740.
- (27)  $n\times$  refers to elongations of  $n$  times the original length of the sample; thus,  $3\times$  is equivalent to 200% elongation.
- (28) Parmer, R. P.; Cobbold, A. J. *Makromol. Chem.* **1964**, *74*, 174–189.

MA9915531